Cancer Microenvironment (2011) 4:73–91
DOI 10.1007/s12307-010-0047-2

ORIGINAL PAPER

Proteomic Analysis of Differentially Expressed Proteins in Peripheral Cholangiocarcinoma

Ian A. Darby · Karine Vuillier-Devillers · Émilie Pinault · Vincent Sarrazy · Sébastien Lepreux · Charles Balabaud · Paulette Bioulac-Sage · Alexis Desmoulière

Received: 17 March 2010 / Accepted: 31 May 2010 / Published online: 26 June 2010

Abstract Cholangiocarcinoma is an adenocarcinoma of the liver which has increased in incidence over the last thirty years to reach similar levels to other liver cancers. Diagnosis of this disease is usually late and prognosis is poor, therefore it is of great importance to identify novel candidate markers and potential early indicators of this disease as well as molecules that may be potential therapeutic targets. We have used a proteomic approach to identify differentially expressed proteins in peripheral cholangiocarcinoma cases and compared expression with paired non-tumoral liver tissue from the same patients. Two-dimensional fluorescence difference gel electrophoresis after labeling of the proteins with cyanines 3 and 5 was used to identify differentially expressed proteins. Overall, of the approximately 2,400 protein spots visualised in each gel, 172 protein spots showed significant differences in expression level between tumoral and non-tumoral tissue with $p<0.01$. Of these, 100 spots corresponding to 138 different proteins were identified by mass spectrometry: 70 proteins were over-expressed whereas 68 proteins were under-expressed in tumoral samples compared to non-tumoral samples. Among the over-expressed proteins, immunohistochemistry studies confirmed an increased expression of 14-3-3 protein in tumoral cells while α-smooth muscle actin and periostin were shown to be overexpressed in the stromal myofibroblasts surrounding tumoral cells. α-Smooth muscle actin is a marker of myofibroblast differentiation and has been found to be a

Ian A. Darby, Karine Vuillier-Devillers, and Émilie Pinault have equally contributed to this work.

I. A. Darby
Cancer and Tissue Repair Laboratory, School of Medical Sciences, RMIT University,
Bundoora, Victoria 3083, Australia

K. Vuillier-Devillers · É. Pinault
Faculté des Sciences et Techniques, Université de Limoges,
UMR 1061 INRA, Institut Fédératif de Recherche 145, Plateau Protéomique,
Limoges F-87060, France

V. Sarrazy · A. Desmoulière
Faculté de Médecine et de Pharmacie, Université de Limoges,
EA 3842, Institut Fédératif de Recherche 145,
Limoges F-87025, France

S. Lepreux · C. Balabaud · P. Bioulac-Sage
Inserm,
U889,
Bordeaux F-33000, France

S. Lepreux · C. Balabaud · P. Bioulac-Sage
Université Victor Segalen Bordeaux 2,
Bordeaux F-33076, France

S. Lepreux · P. Bioulac-Sage
Service d'Anatomie Pathologique, Hôpital Pellegrin,
CHU Bordeaux,
Bordeaux F-33076, France

A. Desmoulière (✉)
Department of Physiology, Faculty of Pharmacy, University of Limoges,
2 rue du Dr. Marcland,
87025 Limoges cedex, France
e-mail: alexis.desmouliere@unilim.fr

prognostic indicator in colon cancer while periostin may also have a role in cell adhesion, proliferation and migration and has been identified in other cancers. This underlines the role of stromal components in cancer progression and their interest for developing new diagnostic or therapeutic tools.

Keywords Cholangiocarcinoma · Myofibroblast · Periostin · α-smooth muscle actin · Tumor stroma

Abbreviations

ACN	Acetonitrile
Cy	Cyanine
DIA	Differential in-gel analysis
DTT	Dithiothreitol
DIGE	Fluorescence difference gel electrophoresis
FA	Formic acid
IPG	Immobilized pH gradient
IDA	Information-dependant acquisition
IEF	Isoelectrofocusing
MS	Mass spectrometry
MMP	Matrix metalloproteinase
SDS	Sodium dodecyl sulfate
PAGE	Polyacrylamide gel electrophoresis
2-D	Two-dimensional
2-DE	Two-dimensional electrophoresis

Introduction

Bile-duct carcinoma (cholangiocarcinoma) which has been generally considered to be less common than hepatocellular carcinoma, has increased in incidence over the last 30 years [1]. In addition, it has very high incidence in some countries where its etiology is linked to parasitic disease of the liver [2]. Cholangiocarcinoma arises from the epithelial cells or cholangiocytes that line bile ducts. The tumor is composed of glandular and tubular structures made of carcinoma cells set in an abundant fibrous stroma. Three main forms of cholangiocarcinoma have been described and categorised based on the position of the tumor in the liver and on the extrahepatic bile duct tree: intrahepatic or peripheral bile-duct carcinoma, hilar adenocarcinoma (Klatskin tumor) and carcinoma of the extrahepatic bile ducts.

Contrary to most cases of hepatocellular carcinoma, the stroma in cholangiocarcinoma is abundant, sclerous, sometimes with calcifications and may be extensive, and submerges the scanty tumoral tubules. The number of modified fibroblasts (myofibroblasts) present is elevated in the intratumoral stroma and is correlated with the degree of tumor fibrosis [3]. Surrounding the tumor, hepatic stellate cells and/or portal fibroblasts also acquire expression of α-smooth muscle actin (αSMA) and seem in direct continuity with intratumoral myofibroblasts [3]. It is well known that these (myo)fibroblastic cells are involved in deposition of extracellular matrix and in matrix remodelling [4]. Stromal cells express matrix metalloproteinase (MMP)-1, MMP-2, MMP-3, MMP-9, or tissue inhibitors of MMPs, TIMP-1 and TIMP-2 [5]. This expression of MMPs and TIMPs is stronger in cholangiocarcinomas that show severe invasion [5]. The stroma surrounding tumoral cells has recently attracted much interest as a factor in tumor growth and metastasis and a possible target for future therapies (for review see [6]). Though several risk factors for developing cholangiocarcinoma have been identified, the pathogenesis of the disease remains poorly understood. Diagnosis of cholangiocarcinoma is often late and patients often have advanced stage disease at the time of diagnosis, leading to a poor clinical outcome. It is therefore important that we understand better the pathogenesis of the disease. In this paper we report the findings of a proteomic study of peripheral cholangiocarcinoma, in comparison with the surrounding non-tumoral tissue, and identify differentially expressed proteins that may play a role in disease development or progression.

In this study we identified several proteins over- or under-expressed in the cholangiocarcinoma tissue compared to normal liver tissue and also looked at the cellular localization of three of these differentially-expressed proteins, 14-3-3 protein, α-SMA and periostin. Two of these (α-SMA and periostin) were expressed in stromal fibroblasts whilst 14-3-3 protein was expressed in cholangiocarcinoma cells. 14-3-3 protein has recently been shown to have a role as an adaptor protein involved in p53 stabilization and thus in regulation of apoptosis [7]. α-SMA is over-expressed in fibrotic tissue and many tumors and has a strong correlation with prognosis in colon cancer for example [8]. Periostin has been detected in several tumor types and has recently been reported to be highly expressed in fibroblasts derived from cholangiocarcinomas and also to correlate with prognosis [9].

With the increased interest in the role of tumor stroma and cancer associated fibroblasts, it is of interest that some of the proteins identified as being differentially expressed were located in the stroma and are markers of myofibroblast differentiation and have been shown to have roles in promoting tumor growth or spread in other cancers.

Materials and Methods

Liver Tissue Samples

Human liver tissue samples used in this study were selected from the files of liver tissue bank of the

Department of Pathology (Pellegrin Hospital, Bordeaux, France). All of the cases included came from resected livers with peripheral cholangiocarcinoma from patients at the University Hospital of Bordeaux during the period 2003–2005. Fourteen patient samples were initially screened by histology (see Table 1) and the four most typical samples were chosen for further proteomic study. The samples on which proteomic analysis was performed consisted of three female and one male patient (mean age of 59.5 years). Brief clinical and pathological characteristics of all patients are summarized in Table 1. Cholangiocarcinoma cases were chosen on the basis that they were of typical morphology and arose on a nearly normal background liver, in general without significant fibrosis or inflammation. Furthermore, serological viral markers were negative.

For all cases, liver tissue specimens were freshly received (within 30–40 min after vascular clamping) and sampled at the Department of Pathology. The specimens of whole tumoral and non-tumoral liver tissue were carefully sampled and representative fragments of tumoral and non-tumoral liver tissue (the latter taken at a distance of at least 2 cm from the tumor) were immediately snap-frozen in liquid nitrogen and stored at −80°C until used for liver protein preparation. Furthermore, the whole tumoral and non-tumoral liver was then fixed in 10% formalin, embedded in paraffin and routinely processed for diagnosis purposes. For immunohistochemistry, samples of tumoral and non-tumoral liver tissue were snap-frozen in isopentane cooled in liquid nitrogen and stored subsequently at −80°C until cryosectioning.

Materials and Reagents for Proteomic Analysis

Isoelectrofocusing (IEF) was carried out on precast 18-cm immobilized pH gradient (IPG) strips (pH 4–7) in an IPGphor II Electrophoresis System (GE Healthcare Bio-Sciences AB, Uppsala, Sweden). Dithiothreitol (DTT) was purchased from Sigma (L'Isle d'Abbeau, France), proteinase inhibitor cocktail tablets were purchased from Roche Diagnostics GmbH (Mannheim, Germany) and other reagents were purchased from GE Healthcare (Orsay, France). All chemical products used for mass spectrometry analysis were purchased from Sigma (St Louis, MO, USA). Sequencing grade modified trypsin used for protein digestion was purchased from Promega (Charbonnières, France).

Preparation of Liver Tissue Protein Samples

Frozen liver tissue samples from either tumors or non-tumoral regions of the liver were placed in liquid nitrogen, and ground thoroughly to a very fine powder with a mortar and pestle. The liver tissue powder (80 to 120 mg) was then homogenized with 5 volumes of lysis buffer (8 M urea, 2 M thiourea, 4% w/v CHAPS, 40 mM Tris, 50 mM DTT, 1 mM EDTA and protease inhibitor cocktail). Liver tissue homogenates were then vortexed, sonicated at 4°C and allowed to sit on ice for 1 h. Crude extracts were centrifuged at 10,000 g for 15 min and the supernatants were purified by precipitation following the manufacturer's instructions described in the Plus One 2D Clean-Up Kit (GE Healthcare Bio-Sciences AB). Precipitates from each of the non-tumoral and tumoral extracts were subsequently solubilized in the solubilization buffer (8 M urea, 2 M thiourea and 4% w/v CHAPS). Determination of protein concentration was performed as described in the PlusOne 2D Quant Kit (GE Healthcare Bio-Sciences AB). The samples were visualized with a 10% sodium dodecyl sulfate (SDS)—polyacrylamide gel electrophoresis (PAGE) to confirm the quality of the protein extraction and protein concentrations.

Cyanine (Cy) Dye Labeling

To perform two-dimensional fluorescence difference gel electrophoresis (2-D DIGE), the experimental strategy was based on minimal labeling with dye swapping. 50 μg tumoral and non-tumoral protein extracts were labeled with Cy3 or Cy5 and the internal standard which was prepared by mixing an equal amount of all tumoral and non-tumoral samples, was labeled with Cy2. Labeling reactions were carried out according to the manufacturer's instructions. Each sample was labeled with 400 pmol of CyDye (GE Healthcare Bio-Sciences AB) on ice for 30 min in the dark and reactions were stopped by adding 1 μl of 10 mM lysine. The CyDye-labeled samples (non-tumoral, tumoral and internal standard) were mixed and added to an equal volume of the solubilization buffer containing 130 mM DTT, 1% v/v IPG buffer and a trace of bromophenol blue.

Two-Dimensional Electrophoresis (2-DE) and Image Analysis

Analytical 2-DE was performed as follows: the CyDye-labeled protein samples were electrophoresed in the first dimension on IPG pH 4–7 gels. After rehydratation at room temperature for 12 h in a reswelling tray (GE Healthcare Bio-Sciences AB), IEF was carried out at 300 V for 750Vh, at 1,000 V for 3,000Vh and at 10,000 V for 65,000Vh in the dark. The gel strips were then equilibrated in 15 ml of the equilibration buffer A (50 mM Tris-HCl pH 8.8, 6 M urea, 30% v/v glycerol, 2% w/v SDS, 50 mM DTT) for 15 min with gentle shaking, and then in 15 ml of the equilibration buffer B (50 mM Tris-HCl pH 8.8, 6 M urea,

Table 1 List and main clinical characteristics of patients involved in the study

Case	Age (years)	Sex	Mode of discovery	Imaging/type of surgery (weight of the removed liver)	Pathology of the tumor	Pathology of the non-tumoral liver
1[a]	47	F	fatigue+raised GGT	7 cm nodule left lobe, left hepatectomy (415 g)	moderately differentiated peripheral cholangiocarcinoma, invading nerves and large portal veins; nodes metastases	secondary biliary fibrosis, mild steatosis
2[a]	70	M	raised GGT	7.5 cm nodule segment V/VI (central), right hepatectomy (823 g)	moderately differentiated peripheral cholangiocarcinoma; invasion of small intratumoral veins	mild portal fibrosis, mild steatosis
3[a]	59	F	raised GGT	9 cm nodule segment IV-V, right hepatectomy+segment IV (800 g)	moderately differentiated peripheral clear cell cholangiocarcinoma, invading nerves, large portal veins and focally biliary gallbladder	subnormal
4[a]	62	F	abdominal pain+raised GGT	12 cm nodule poorly limited right lobe, right hepatectomy (704 g)	moderately/poorly differentiated peripheral cholangiocarcinoma, invading nerves, small intratumoral veins, biliary channels and Glisson's capsule	subnormal
5	65	M	raised GGT	6 cm nodule segment II/III, left hepatectomy (300 g)	well-differentiated peripheral cholangiocarcinoma+daughter nodules, invading hilar fat, nerves and portal veins	mild portal fibrosis+marked inflammatory infiltrate; 20% steatosis
6	74	F	raised GGT; dilatation of IHBD	3.5 cm nodule segment IV, left hepatectomy (325 g)	well-differentiated peripheral cholangiocarcinoma, invading hilar fat, nerves and portal veins	mild portal fibrosis; 25% steatosis
7	78	F	abdominal pain	7 cm nodule segment IV/V, left hepatectomy+V (325 g)	moderately/poorly differentiated peripheral cholangiocarcinoma, invading intratumoral veins + 1 node	secondary biliary fibrosis, mild steatosis (10%); vascular changes+NRH (secondary to previous chemotherapy)
8	66	M	abdominal pain	5.5 cm nodule segment III, left hepatectomy (460 g)	moderately differentiated peripheral cholangiocarcinoma+daughter nodules, invading Glisson's capsule, hilar fat, nerves, bile ducts, veins and lymphatics + 2 metastatic nodes	marked portal inflammation+secondary biliary fibrosis, 30% steatosis
9	54	F	abdominal pain+mass syndrome	8 cm nodule segment IV, central hepatectomy (306 g)	moderately differentiated peripheral cholangiocarcinoma+daughter nodules, invasion of intratumoral veins	subnormal
10	71	F	fortuitous discovery of a left liver tumor by echography in 2001: diagnosis of hemangioma	8.5 cm nodule segment II/III/IV, left hepatectomy (575 g)	well/moderately differentiated peripheral cholangiocarcinoma+daughter nodules, invasion of portal veins	atrophy
11	68	M	raised GGT; wasting	8 cm nodule segment VI/VII, lateral right hepatectomy (760 g)	moderately differentiated peripheral cholangiocarcinoma with small hepatoid component (hepatocholangiocarcinoma)+ daughter nodules, portal vascular and endobiliary invasion	atrophy, septal fibrosis and changes secondary to bile duct obstruction
12	67	F	pain	6.5 cm nodule segment VI/VII, right hepatectomy (892 g)	moderately differentiated peripheral cholangiocarcinoma with+daughter nodules, portal veins and nerves invasion	mild portal fibrosis; 25% steatosis
13	78	M	raised GGT	5.5 cm nodule segment IV, median hepatectomy (400 g)	well differentiated peripheral cholangiocarcinoma	congenital hepatic fibrosis, 15% steatosis
14	41	M		9.5 cm nodule segment VII, right hepatectomy (848 g)	sclerosing cavernous hemangioma	subnormal

GGT gamma glutamyl transpeptidase; *NRH* nodular regenerative hyperplasia

[a] patients that were used for the proteomic study

30% v/v glycerol, 2% w/v SDS, 2.5%w/v iodoacetamide, with a trace of bromophenol blue). The equilibrated strips were loaded on to the top of 10% SDS-PAGE (24x20 cm) and sealed with 1% w/v agarose. Separation in the second dimension was carried out in Tris-glycine buffer [10]. After 2-DE, gels were scanned with a Typhoon TRIO scanner (GE Healthcare Bio-Sciences AB) using filters appropriate for each dye's excitation and emission wavelength. To obtain an adequate amount of the proteins from the individual spots for identification, 400 μg of the tumoral samples and 400 μg of the non-tumoral samples were separately run on 2D electrophoresis and were stained using a colloidal CBB G-250 procedure [11]. Preparative gels were scanned with an Image Scanner II (GE Healthcare Bio-Sciences AB).

Statistical Analysis

After the images were scanned, GE Healthcare DeCyder software 5.01 was used for differential gel analysis. The 2-D image of tumoral liver tissue was compared with that of the non-tumoral liver tissue *via* the internal standard sample. Specifically the protein expression analysis was performed for each of the four gels in parallel using the differential in-gel analysis (DIA) module of DeCyder using a value of 2,500 as the initial estimate of protein spots present. DIA analysis allows for the direct comparison of intensities of specific protein spots between different samples within the same gel. In this case, protein intensities were compared between the tumoral proteome and non-tumoral proteome. These DIA analyses were collated into a single analysis using the biological variation analysis module of DeCyder, and final values for the expression ratio of specific protein spots between tumoral liver tissue and non-tumoral liver tissue were determined for >2 or <−2 fold differences. The statistical significance of each expression level was calculated using Student's *t* test on the logged ratio. Results obtained by DeCyder software were compared to those obtained with Progenesis SameSpot software (version 3.2, Nonlinear Dynamics). Significantly differentially expressed spots between tumoral and non-tumoral tissue were selected using a type one error risk of 1%, at least a power of 80% and that they were found on all the images.

Digestion of Proteins

Protein spots were excised from 2-DE gels that had been stained with Coomassie blue G-250. The excised spots were first destained by washing in milliQ distilled water then dehydrated in 50 μl of acetonitrile (ACN) followed by rehydration in 50 μl of 100 mM ammonium bicarbonate for 15 min at 37°C. An equivalent volume of ACN was then added to the mix and further incubated for 15 min at 37°C. Samples were then dried by vacuum dessicator. Sequencing grade modified trypsin was prepared from a stock solution at 0.1 μg/μl and diluted in 25 mM ammonium bicarbonate to a final concentration of 10 ng/μl. Dehydrated spots were incubated in 25 μl of trypsin at 10 ng/μl (a total of 250 ng per spot) overnight at 37°C. The supernatant was then collected in a 0.5 ml microfuge tube and the digested peptides extracted sequentially in 50 μl of 40% ACN—1% formic acid (FA), then 10 μl of 25% ACN—1% FA and finally 25 μl of 60% ACN. All samples were then dried by evaporation using a vacuum dessicator.

Mass Spectrometry (MS)

After trypsin digestion and evaporation, the peptides were resolubilised in 6 μl of Switchos solvent (2% ACN, 0.05% TFA) for analysis by nano-LC MS/MS using a nano-chromatography liquid LC Packings system (Dionex, Amsterdam, Holland) coupled to a 2000-QTRAP mass spectrometer (Applied Biosystems, Courtaboeuf, France). For each sample, 5 μl was injected into a pre-column (C18 Pepmap^{TM} 300 μm ID x 5 mm) using the Switchos unit. After desalting for 3 min with Switchos solvent, the pre-column was switched online with the analytical column (C18 Pepmap^{TM} 75 μm ID x 150 mm) pre-equilibrated with 100% solvent A (2% ACN—0.1% FA). Peptides were eluted from the pre-column into the analytical column and then into the mass spectrometer by a linear gradient of 0% to 50% of solvent B (90% ACN—0.1% FA) over 65 min at a flow rate of 300 nl/min.

Data acquisition was carried out using the IDA (Information-Dependant Acquisition) software of Analyst 1.4.2 (Applied Biosystems). The data from MS and MS/MS were continuously recorded with a cycle duration of 3 sec. For each MS scan, two precursors were selected for fragmentation on the basis of their intensity (greater than 20,000 cps), their charge state (2+, 3+) and if the precursor had already been selected for fragmentation (dynamic exclusion). The collision energies were automatically adjusted according to the charge state and ionic mass of selected precursors.

Peptide Identification

For protein identification, the results of analysis by nano-LC MS/MS were used to search the SwissProt database (Swiss-Prot Release 51.6, 6 February 2007, 257 964 sequences) using the Mascot software (version 2.2, Matrix Science, UK) with the following criteria: species *Homo sapiens*, 0.5 Da tolerance for peptide and peptide fragment mass, a single missed cleavage site allowed during trypsin digestion, and carbamidomethylation of cysteine residues

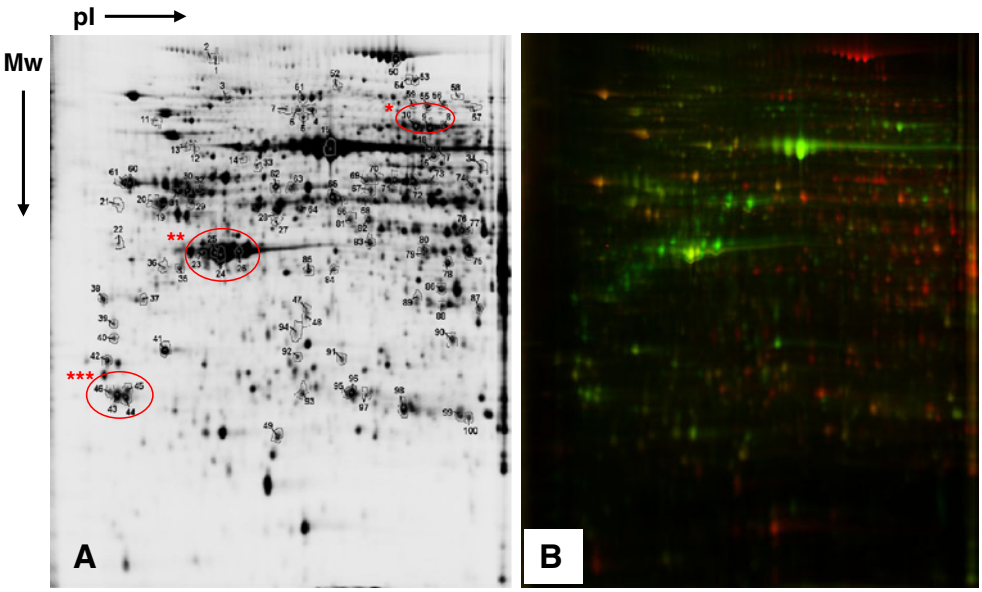

Fig. 1 2-D DIGE gel images. The image A shows the internal standard master. Indicated numbers correspond to identified spots (refer to Tables 2 and 3). The three proteins selected for further analyses are marked with * (periostin), ** (smooth muscle actin) and *** (14-3-3 isoforms). The image B associates Cy3-labeled non-tumoral sample image (*red*) with Cy5-labeled tumoral sample image (*green*). 2-DE was performed using a pH range of 4-7 in the first dimension and SDS-PAGE (10%) in the second

(due to alkylation of -SH groups by iodoacetamide) and oxidation of methionine as variable modifications. Protein identification was validated if at least 2 peptides had a score of greater than 25, or one peptide had a score of greater than 50 at a confidence level of at least 95%.

Western Blot

6 μg from each protein sample extracted for 2-DE analysis was run on a 10% SDS-polyacrylamide gel and transferred to a nitrocellulose membrane (Hybond ECL, GE Healthcare, Orsay, France). The membrane was blocked in TBST buffer (20 mM Tris-HCl pH 7.6, 137 mM NaCl, 0.1% Tween 20) containing 1% blocking buffer (Roche Diagnostics, Meylan, France) before adding the periostin [osteoblast specific factor-2] antibody (rabbit polyclonal, BioVendor, Heidelberg, Germany) at a 1:10,000 dilution in TBST buffer with 0.5% blocking buffer. Membranes were incubated overnight at 4°C. After washing, the membranes were incubated with a secondary peroxidase-conjugated swine anti-rabbit antibody (1:1,000 in TBST buffer with 0.5% blocking buffer). Signal was detected with a BM chemiluminescence blotting kit (Roche).

Immunohistochemistry

All samples had tissue embedded for frozen sectioning. This tissue was taken from the periphery of the tumor sample so that it contained both tumor tissue and non-tumoral liver which was histologically normal. Liver samples snap-frozen in isopentane/liquid nitrogen were sectioned on a cryostat at 5 μm, fixed for 5 min in 4% paraformaldehyde and then stained by immunohistochemistry using primary antibodies directed against α-smooth muscle actin (mouse mAb, Dako, Carpinteria, USA), periostin [osteoblast specific factor-2] (rabbit polyclonal, BioVendor, Heidelberg, Germany) and 14-3-3 B/a protein (rabbit mAb, Novus Biologicals, Littleton, USA). Detection of labeling was carried out using Alexa-labeled secondary antibodies; Alexa 594 goat-anti mouse IgG (Invitrogen SARL, Cergy Pontoise, France) and Alexa 488 goat anti-rabbit IgG (Invitrogen). Slides were mounted in aqueous mounting medium (Dako, Carpinteria, USA) for viewing and photography. For staining by immunoperoxidase, incubation in the primary antibody was followed by incubation in secondary antibodies linked to HRP (Envision™ + system, Dako) and the positive staining was detected using diaminobenzidine. Slides were counter-stained with hematoxylin for viewing and photomicroscopy. Specificity of staining was confirmed by incubation in non-immune serum and in the absence of the primary antibody.

Results

Identification of Differentially Expressed Proteins

Analysis of 2-D gels showed that there were approximately 2,400 spots detected on protein samples from 8 biopsies from four patients (Fig. 1). Of these, analysis using DIGE showed that 172 protein spots exhibited significant variations (at least 2-fold changes) at a $p<0.01$ confidence level and at least a power of 80%. 49 protein spots were up-regulated in the tumoral liver tissue compared to the non-tumoral liver tissue. Nano-LC MS/MS analysis of these spots led to the identification of 70 different proteins. Among 123 down-regulated protein spots, 51 spots corresponding to 68

Table 2 Under-expressed proteins

Swiss Prot ID[a]	Identified Protein[a]	Theor. MW/pI[b]	SSP[c]	Av. ratio[d]	Protein score[e]	Matched peptides	Sequence coverage (%)	Bibliographic references[f]
Metabolism								
FTHFD_HUMAN	10-formyltetrahydrofolate dehydrogenase	98767/5.63	51	−13.44	1167	52	46.1%	[45]
D3D2_HUMAN	3,2-trans-enoyl-CoA isomerase, mitochondrial precursor	32795/8.80	97	−5.07	54	1	4.3%	
3HIDH_HUMAN	3-hydroxyisobutyrate dehydrogenase, mitochondrial precursor	35306/8.38	92	−4.97	300	9	28.9%	
HPPD_HUMAN	4-hydroxyphenylpyruvate dioxygenase	44906/6.52	75	−6.06	258	13	23.9%	
			79	−9.12	224	8	19.8%	
AL9A1_HUMAN	4-trimethylaminobutyraldehyde dehydrogenase	53767/5.69	64	−4.43	303	11	22.5%	
AAKG1_HUMAN	5∼-AMP-activated protein kinase subunit gamma-1	37556/6.42	89	−3.75	72	1	3%	
ADK_HUMAN	Adenosine kinase	40520/6.24	79	−9.12	107	5	13.5%	
SAHH_HUMAN	Adenosylhomocysteinase	47685/5.92	83	−3.46	586	20	28.9%	
ARK73_HUMAN	Aflatoxin B1 aldehyde reductase member 3	37183/6.67	87	−6.92	407	15	31.1%	[46]
AK1A1_HUMAN	Alcohol dehydrogenase [NADP+]	36550/6.32	86	−4.7	264	20	46.8%	[12]
			87	−6.92	79	3	14.2%	
ALDH2_HUMAN	Aldehyde dehydrogenase, mitochondrial precursor	56346/6.63	65	−10.79	354	28	48.5%	[12]
			66	−8.425	480	16	30.8%	
			68	−5.6	591	15	29.4%	
			85	−12.34	170	5	11%	
AK1C4_HUMAN	Aldo-keto reductase family 1 member C4	37071/6.71	89	−3.75	75	2	5.3%	
ALDR_HUMAN	Aldose reductase	35830/6.51	86	−4.7	62	2	3.2%	
ARGI1_HUMAN	Arginase-1	34713/6.72	86	−4.7	82	2	9%	[47]
ST2A1_HUMAN	Bile salt sulfotransferase	33758/5.71	94	−9.17	273	12	39.3%	
PYR1_HUMAN	CAD protein	242829/6.02	50	−30.19	60	4	1.2%	
CPSM_HUMAN	Carbamoyl-phosphate synthase [ammonia], mitochondrial precursor	164835/6.30	50	−30.19	1860	101	56.3%	[13]
CGL_HUMAN	Cystathionine gamma-lyase	44479/6.21	79	−9.12	287	9	27.2%	[48]
			80	−7.1	95	2	5.9%	
CNDP2_HUMAN	Cytosolic nonspecific dipeptidase	52845/5.66	65	−10.79	69	2	6.1%	
HEM2_HUMAN	Delta-aminolevulinic acid dehydratase	36271/6.32	88	−7.54	150	4	12.1%	
			89	−3.75	68	2	6.1%	
DHPR_HUMAN	Dihydropteridine reductase	25773/6.90	100	−4.9	355	10	37.3%	
DPYS_HUMAN	Dihydropyrimidinase	56594/6.81	82	−11.29	91	3	6.4%	
ENTP5_HUMAN	Ectonucleoside triphosphate diphosphohydrolase 5 precursor	47487/5.92	83	−3.46	241	7	18%	
EFTU_HUMAN	Elongation factor Tu, mitochondrial precursor	49510/7.26	75	−6.06	62	1	2.7%	
ECHM_HUMAN	Enoyl-CoA hydratase, mitochondrial precursor	31367/8.34	93	−11.65	459	13	35.2%	
			95	−11.09	606	18	40.7%	
			96	−7.97	643	19	39.7%	
			97	−5.07	424	10	32.4%	
HYES_HUMAN	Epoxide hydrolase 2	62575/5.91	69	−9.42	202	7	11.9%	[49]
FTCD_HUMAN	Formimidoyltransferase-cyclodeaminase	58889/5.58	62	−14.77	389	23	35.9%	
F16P1_HUMAN	Fructose-1,6-bisphosphatase 1	36791/6.54	76	−8.23	67	2	8.9%	
FAAA_HUMAN	Fumarylacetoacetase	46344/6.46	78	−11.86	350	13	27.4%	
			79	−9.12	91	2	6.9%	
GLSL_HUMAN	Glutaminase liver isoform, mitochondrial precursor	66267/6.56	72	−11.62	98	2	4.2%	
GATM_HUMAN	Glycine amidinotransferase, mitochondrial precursor	48424/8.26	76	−8.23	251	13	26.5%	
			77	−9.85	218	7	15.6%	
GNMT_HUMAN	Glycine N-methyltransferase	32721/6.55	90	−12.82	336	8	27.5%	

Table 2 (continued)

Swiss Prot ID[a]	Identified Protein[a]	Theor. MW/pI[b]	SSP[c]	Av. ratio[d]	Protein score[e]	Matched peptides	Sequence coverage (%)	Bibliographic references[f]
PYGL_HUMAN	Glycogen phosphorylase, liver form	97087/6.71	56	−7.6	56	1	1.1%	
GRHPR_HUMAN	Glyoxylate reductase/hydroxypyruvate reductase	35646/7.01	88	−7.54	175	12	25.9%	
			89	−3.75	98	2	7.9%	
HMCS1_HUMAN	Hydroxymethylglutaryl-CoA synthase, cytoplasmic	57257/5.22	77	−9.85	62	1	2.1%	
HMCS2_HUMAN	Hydroxymethylglutaryl-CoA synthase, mitochondrial precursor	56599/8.40	76	−8.23	148	4	8.1%	
HPRT_HUMAN	Hypoxanthine-guanine phosphoribosyltransferase	24564/6.21	98	−2.99	187	4	21.1%	
IDHC_HUMAN	Isocitrate dehydrogenase [NADP] cytoplasmic	46630/6.53	75	−6.06	308	25	45.9%	
KHK_HUMAN	Ketohexokinase	32710/5.64	91	−9.73	231	6	18.1%	
EST1_HUMAN	Liver carboxylesterase 1 precursor	62481/6.15	69	−9.42	309	10	15.9%	
			70	−8.73	485	16	29.6%	
			71	−7.18	462	15	24.3%	
			72	−11.62	419	21	37.7%	
			73	−6.48	255	9	17.5%	
MDHC_HUMAN	Malate dehydrogenase, cytoplasmic	36403/6.91	87	−6.92	261	7	25.4%	
MCCB_HUMAN	Methylcrotonoyl-CoA carboxylase beta chain, mitochondrial precursor	61294/7.57	74	−4.53	319	12	21%	
GANAB_HUMAN	Neutral alpha-glucosidase AB precursor	106807/5.74	52	−6.4	425	20	19.2%	
NLTP_HUMAN	Nonspecific lipid-transfer protein	58956/6.44	81	−5.01	200	11	11.9%	
PRDX6_HUMAN	Peroxiredoxin-6	25019/6.00	96	−7.97	81	3	20.1%	
			98	−2.99	367	14	29%	
			99	−2.07	102	3	13.4%	
PH4H_HUMAN	Phenylalanine-4-hydroxylase	51829/6.15	82	−11.29	88	3	5.1%	
PCYOX_HUMAN	Prenylcysteine oxidase precursor	56604/5.80	67	−3.14	134	5	11.5%	
PDIA3_HUMAN	Protein disulfide-isomerase A3 precursor	56747/5.98	62	−14.77	114	3	6.7%	
			63	−2.24	502	18	33.3%	
PDIA1_HUMAN	Protein disulfide-isomerase precursor	57081/4.76	60	−2.25	512	24	40.7%	
			61	−3.46	626	26	35.8%	
PNPO_HUMAN	Pyridoxine-5∼-phosphate oxidase	29969/6.62	97	−5.07	152	4	18%	
PYC_HUMAN	Pyruvate carboxylase, mitochondrial precursor	129551/6.37	53	−9.58	626	28	28.2%	
			54	−6.4	135	6	5.7%	
KPYR_HUMAN	Pyruvate kinase isozymes R/L	61791/7.64	73	−6.48	111	5	10.3%	
AL1A1_HUMAN	Retinal dehydrogenase 1	54827/6.30	73	−6.48	520	14	29.9%	
METK1_HUMAN	S-adenosylmethionine synthetase isoform type-1	43620/5.86	81	−5.01	97	2	6.1%	[50]
			82	−11.29	138	8	20.5%	
SARDH_HUMAN	Sarcosine dehydrogenase, mitochondrial precursor	100973/6.80	57	−12.75	51	5	3.5%	
SBP1_HUMAN	Selenium-binding protein 1	52280/6.13	65	−10.79	174	7	17.2%	[14, 15]
			66	−8.425	455	11	25.2%	
			68	−5.6	58	1	2.1%	
SDSL_HUMAN	Serine dehydratase-like	34652/6.41	86	−4.7	126	5	20.1%	
ACDSB_HUMAN	Short/branched chain specific acyl-CoA dehydrogenase, mitochondrial precursor	47455/6.53	84	−9.21	468	14	39.4%	
			85	−12.34	327	11	28.2%	
TALDO_HUMAN	Transaldolase	37516/6.36	89	−3.75	124	3	10.4%	
TPIS_HUMAN	Triosephosphate isomerase	26653/6.45	99	−2.07	500	11	48.6%	
GALE_HUMAN	UDP-glucose 4-epimerase	38257/6.26	89	−3.75	157	4	8.6%	
UGDH_HUMAN	UDP-glucose 6-dehydrogenase	54989/6.73	74	−4.53	437	11	20.6%	
VATB2_HUMAN	Vacuolar ATP synthase subunit B, brain isoform	56465/5.57	63	−2.24	65	1	2.9%	
Cell cycle								
CN166_HUMAN	Protein C14orf166	28051/6.19	98	−2.99	122	3	15.2%	

Table 2 (continued)

Swiss Prot ID[a]	Identified Protein[a]	Theor. MW/pI[b]	SSP[c]	Av. ratio[d]	Protein score[e]	Matched peptides	Sequence coverage (%)	Bibliographic references[f]
Cytoskeleton								
ACTH_HUMAN	Actin, gamma-enteric smooth muscle	41850/5.31	75	−6.06	68	2	7.7%	
Heat shock proteins								
HSPB1_HUMAN	Heat-shock protein beta-1	22768/5.98	96	−7.97	196	7	31.7%	[51]
RNA binding								
IREB1_HUMAN	Iron-responsive element-binding protein 1	98337/6.23	55	−5.97	160	12	11.5%	
			59	−8.00	54	2	1.8%	
Signalling								
ERBB2_HUMAN	Receptor tyrosine-protein kinase erbB-2 precursor	137821/5.58	86	−4.7	55	1	0.9%	
Non identified			58	−2.58				

[a] Accession numbers of proteins and protein name from Swiss-Prot databases

[b] Theoretical molecular weight and isoelectric point obtained from Swiss-Prot and the ExPASy databases (http://au.expasy.org)

[c] Sample spot number (SSP) refers to numbering in Fig. 1

[d] Av. ratio refers to the ratio of normalized spot intensities of tumoral and non-tumoral tissues. A positive ratio indicates over-expression in the tumor, whereas a negative ratio indicates a reduced expression in the tumor

[e] Mascot score for the identified proteins based on the peptide ion score with a confidence level of at least 95% (http://www.matrixscience.com)

[f] Bibliographic reference for proteins already described in carcinogenesis or liver pathology by transcriptomic, proteomic or specific studies

different proteins were identified. The list of proteins that were found to be under-expressed or over-expressed in the tumoral liver tissue compared with the non-tumoral liver tissue, are shown respectively in Table 2 and Table 3. The expression ratios of these proteins and their Swiss-Prot identification numbers are also specified.

Proteins Under-Expressed in the Tumoral Liver Tissue Compared with the Non-Tumoral Liver Tissue

The proteins that were found to be under-expressed in the tumoral liver tissue compared with the non-tumoral liver tissue are shown in Table 2. Many of these proteins were involved in cellular metabolism while a number were cytoskeletal proteins. Several of these proteins have also been reported to be differentially expressed in either hepatocellular carcinoma or other tumor types, for example alcohol dehydrogenase and aldehyde dehydrogenase [12], carbamyl phosphate synthase [13], selenium binding protein 1 and DNA helicase RuvB-like protein 2 ([14–16]).

Proteins Over-Expressed in the Tumoral Liver Tissue Compared with the Non-Tumoral Liver Tissue

As shown in Table 3, proteins that were found to be over-expressed in the tumoral liver tissue compared with the non-tumoral liver tissue could be categorised by functions into several groups including cytoskeletal proteins, apoptosis/survival and cellular metabolism. Some of the proteins identified have been reported to be differentially expressed in hepatocellular carcinoma, for example elongation factor 1 delta, ERO-1 like protein and ezrin ([17–19]). Proteomic screening confirmed the over-expression of several proteins that have previously been shown by other methods to be highly expressed in tumor or tumoral stroma. An example of one of these proteins was α-smooth muscle actin, a marker of stromal cell activation that has been linked to poor prognosis in colon cancer [8] and is present in stromal myofibroblasts in several tumor types [3]. The proteomic screen also showed over-expression of novel proteins such as the 14-3-3 proteins which are phospho-serine/phosphothreonine-binding proteins that may promote cell survival and have been suggested to be a possible target for therapies aimed at enhancing killing of cancer cells [20]. Other proteins that were over-expressed and could be postulated to have a link to tumorigenesis or cancer growth or spread included pigment epithelium derived factor precursor, a potent anti-angiogenic protein that has the potential to limit tumor growth [21]. Interestingly, we also found increased expression of periostin in the tumoral liver tissue compared to non-tumoral liver tissue and this protein has been described in other tumor types for example breast cancers, melanoma and colon cancers ([22–24]). The elevation of these proteins in tumoral liver tissue versus non-tumoral liver tissue was also shown to

Table 3 Over-expressed proteins

Swiss Prot ID[a]	Identified Protein[a]	Theor. MW/pI[b]	SSP[c]	Av. ratio[d]	Protein score[e]	Matched peptides	Sequence coverage (%)	Bibliographic references[f]
Apoptosis/survival								
1433B_HUMAN	14-3-3 protein beta/alpha	28065/4.76	44	2.25	515	17	57.3%	[20, 39, 52]
			45	2.43	306	12	34.6%	
1433F_HUMAN	14-3-3 protein eta	28201/4.76	43	4.4	143	6	21.1%	
			45	2.43	159	9	18.3%	
			44	2.25	215	10	33.7%	
1433G_HUMAN	14-3-3 protein gamma	28285/4.8	43	4.4	131	4	15%	
			45	2.43	458	19	55.5%	
			44	2.25	341	11	31.6%	
1433S_HUMAN	14-3-3 protein sigma	27757/4.68	44	2.25	124	5	10.5%	
			45	2.43	140	4	10.5%	
			46	3.06	152	5	10.5%	
1433T_HUMAN	14-3-3 protein theta	27747/4.68	46	3.06	624	19	55.9%	
			43	4.4	170	5	20%	
1433Z_HUMAN	14-3-3 protein zeta/delta	27728/4.73	43	4.4	328	11	38%	[40, 41, 53]
			44	2.25	233	8	28.6%	
			45	2.43	370	11	41.6%	
			46	3.06	322	10	33.9%	
ANXA5_HUMAN	Annexin A5	35914/4.94	41	3.31	570	30	52.5%	[29]
Ribosomal protein								
RLA0_HUMAN	60 S acidic ribosomal protein P0	34252/5.71	47	5.44	141	4	13.6%	[27, 54]
Heat shock proteins								
GRP78_HUMAN	78 kDa glucose-regulated protein precursor	72288/5.07	20	2.34	63	3	3.8%	
Coagulation								
FIBG_HUMAN	Fibrinogen gamma chain precursor	51479/5.37	28	2.12	155	6	19%	
THRB_HUMAN	Prothrombin precursor	69992/5.64	11	2.68	415	14	29.1%	
Cytoskeleton								
ACTA_HUMAN	Actin, aortic smooth muscle	41982/5.23	25	4.43	523	21	49.6%	[3, 55]
ACTB_HUMAN	Actin, cytoplasmic 1	41710/5.29	25	4.43	431	20	48%	
ACTG_HUMAN	Actin, cytoplasmic 2	41766/5.31	23	2.78	322	20	51.7%	
			24	2.52	1187	73	57.6%	
			26	2.72	723	28	56.5%	
ACTN4_HUMAN	Alpha-actinin-4	104788/5.27	3	2.15	481	20	21.3%	[28]
DESM_HUMAN	Desmin	53503/5.21	22	3.13	96	4	8.1%	[56]
			31	3.45	100	6	9.1%	
EZRI_HUMAN	Ezrin	69370/5.94	10	4.01	55	4	6.3%	[19]
GELS_HUMAN	Gelsolin precursor	85644/5.9	4	6.6	499	16	19.8%	[57]
			6	5.27	743	20	26.7%	
			7	5.2	378	13	20.7%	
K1C19_HUMAN	Keratin, type I cytoskeletal 19	44065/5.04	35	15.9	819	33	57%	[58]
			36	14.91	900	29	58%	
LMNA_HUMAN	Lamin-A/C	74095/6.57	16	2.29	86	2	2.7%	
			17	6.36	77	1	1.4%	
LMNB2_HUMAN	Lamin-B2	67647/5.29	14	2.06	317	13	19.2%	[59]
MOES_HUMAN	Moesin	67778/6.08	10	4.01	129	9	13.2%	
PERI_HUMAN	Peripherin	53618/5.37	22	3.13	129	6	8.3%	
			31	3.45	163	6	8.5%	
RADI_HUMAN	Radixin	68521/6.03	10	4.01	94	5	8.1%	[58]

Table 3 (continued)

Swiss Prot ID[a]	Identified Protein[a]	Theor. MW/pI[b]	SSP[c]	Av. ratio[d]	Protein score[e]	Matched peptides	Sequence coverage (%)	Bibliographic references[f]
TPM3_HUMAN	Tropomyosin alpha-3 chain	32799/4.68	39	16.79	50	2	6.7%	
			40	19.8	70	2	6.7%	
			38	12.49	211	10	19%	
TPM4_HUMAN	Tropomyosin alpha-4 chain	28504/4.67	40	19.8	54	2	12.1%	
			42	4.93	226	10	36.3%	
			38	12.49	316	17	21.8%	
TPM2_HUMAN	Tropomyosin beta chain	32831/4.66	38	12.49	577	23	31%	
			42	4.93	119	4	13.4%	
TPM1_HUMAN	Tropomyosin-1 alpha chain	32689/4.69	38	12.49	353	10	16.9%	
			39	16.79	103	4	13.7%	
			40	19.8	183	6	19%	
TBA1_HUMAN	Tubulin alpha-1 chain	49892/4.95	29	2.04	507	18	47.5%	
			30	2.44	567	19	38.4%	
			31	3.45	342	13	27.7%	
			32	3.69	226	8	20.1%	
TBA3_HUMAN	Tubulin alpha-3 chain	50104/4.94	29	2.04	586	21	53%	
			30	2.44	494	20	40.4%	
			31	3.45	426	14	31.3%	
			32	3.69	303	11	26.8%	
TBA6_HUMAN	Tubulin alpha-6 chain	49863/4.96	30	2.44	315	18	35.2%	
TBA8_HUMAN	Tubulin alpha-8 chain	50062/4.94	30	2.44	343	12	21.4%	
			31	3.45	207	9	19.2%	
			29	2.04	342	13	30.7%	
			32	3.69	136	5	13.1%	
TBAK_HUMAN	Tubulin alpha-ubiquitous chain	50120/4.94	30	2.44	524	21	40.4%	
			31	3.45	480	16	34.1%	
			32	3.69	388	12	29.7%	
			29	2.04	663	23	55.9%	
TBB5_HUMAN	Tubulin beta chain	49639/4.78	19	2.31	1128	59	59.2%	[26]
			20	2.34	1354	41	59%	
TBB1_HUMAN	Tubulin beta-1 chain	50295/5.05	19	2.31	251	13	8.4%	
TBB2A_HUMAN	Tubulin beta-2A chain	49875/4.78	19	2.31	834	54	57.1%	
			20	2.34	1066	35	58.9%	
TBB2C_HUMAN	Tubulin beta-2C chain	49799/4.79	19	2.31	1053	53	59.1%	
			20	2.34	1213	38	58.9%	
TBB3_HUMAN	Tubulin beta-3 chain	50400/4.83	19	2.31	824	38	42.7%	
			20	2.34	832	23	37.3%	
TBB4_HUMAN	Tubulin beta-4 chain	49554/4.78	19	2.31	993	44	53.8%	
			20	2.34	979	29	53.6%	
TBB4Q_HUMAN	Tubulin beta-4q chain	48403/5.11	19	2.31	295	16	16.4%	
TBB6_HUMAN	Tubulin beta-6 chain	49825/4.77	19	2.31	716	38	43.7%	
			20	2.34	660	23	41.5%	
VIME_HUMAN	Vimentin	53619/5.06	19	2.31	351	13	27%	
			20	2.34	68	2	4.1%	
			22	3.13	735	27	54.1%	
			30	2.44	186	5	9.9%	
			32	3.69	247	9	21.9%	
			29	2.04	313	9	20.4%	
			31	3.45	1263	35	64.8	

Table 3 (continued)

Swiss Prot ID[a]	Identified Protein[a]	Theor. MW/pI[b]	SSP[c]	Av. ratio[d]	Protein score[e]	Matched peptides	Sequence coverage (%)	Bibliographic references[f]
WDR1_HUMAN	WD repeat protein 1	66152/6.17	16	2.29	492	20	32%	
Protease inhibitor								
A1AT_HUMAN	Alpha-1-antitrypsin precursor	46707/5.37	29	2.04	105	3	8.4%	[60]
			31	3.45	551	27	51.2%	
			32	3.69	97	3	8.6%	
AMBP_HUMAN	AMBP protein precursor	38974/5.95	41	3.31	99	3	12.5%	[61]
DNA binding								
KU86_HUMAN	ATP-dependent DNA helicase 2 subunit 2	82652/5.55	5	2.07	610	36	47.5%	[62]
RBBP4_HUMAN	Histone-binding protein RBBP4	47626/4.74	21	2.48	178	9	17.9%	[33]
RUVB2_HUMAN	RuvB-like 2	51125/5.49	28	2.12	968	27	57.2%	[16]
HNRPK_HUMAN	Heterogeneous nuclear ribonucleoprotein K	50944/5.39	33	2.24	508	18	35.6%	
Metabolism								
CERU_HUMAN	Ceruloplasmin precursor	122128/5.44	1	3.04	477	15	16.6%	
			2	3.00	444	14	14.1%	
CBS_HUMAN	Cystathionine beta-synthase	60548/6.2	18	7.57	113	6	9.8%	[63]
EF1D_HUMAN	Elongation factor 1-delta	31103/4.9	37	2.92	114	2	8.5%	[17]
ERO1A_HUMAN	ERO1-like protein alpha precursor	54358/5.48	33	2.24	95	5	12%	[17, 18]
PGTA_HUMAN	Geranylgeranyl transferase type-2 alpha subunit	65030/5.46	33	2.24	354	12	22.6%	
GSTP1_HUMAN	Glutathione S-transferase P	23341/5.43	49	4.4	478	19	58.1%	[31, 64]
GPDA_HUMAN	Glycerol-3-phosphate dehydrogenase [NAD+], cytoplasmic	37569/5.81	47	5.44	52	1	2.6%	[32]
LDHB_HUMAN	L-lactate dehydrogenase B chain	36615/5.71	47	5.44	704	26	53.9%	[36]
			48	7.2	767	25	52.1%	
PPCKM_HUMAN	Phosphoenolpyruvate carboxykinase [GTP], mitochondrial precursor	70592/7.56	18	7.57	96	4	6.7%	[65]
VA0D_HUMAN	Vacuolar ATP synthase subunit d	40303/4.89	37	2.92	112	5	19.7%	
DFNA5_HUMAN	Non-syndromic hearing impairment protein 5	54520/5.03	31	3.45	60	2	4.2%	[38]
SC23B_HUMAN	Protein transport protein Sec23B	86424/6.43	8	6.06	51	3	3.3%	
Immunity								
CO9_HUMAN	Complement component C9 precursor	63133/5.43	12	4.97	410	19	29.9%	
			13	6.15	168	8	15%	
ILF2_HUMAN	Interleukin enhancer-binding factor 2	43035/5.19	26	2.72	296	7	16.7%	
Extracellular matrix								
LUM_HUMAN	Lumican precursor	38405/6.16	20	2.34	87	3	10.7%	[66]
POSTN_HUMAN	Periostin precursor	93255/7.27	8	6.06	1049	32	40%	[22–24, 67, 68]
			9	6.21	426	12	16.1%	
			10	4.01	864	29	34.4%	
Tumour marker								
NIBL_HUMAN	Niban-like protein	82631/5.81	4	6.6	82	3	5.6%	[37]
Nuclear protein								
NPM_HUMAN	Nucleophosmin	32555/4.64	37	2.92	249	7	23.5%	[34]
SMCE1_HUMAN	SWI/SNF-related matrix-associated actin-dependent regulator of chromatin subfamily E member 1	46621/4.85	19	2.31	114	2	5.6%	
			20	2.34	89	2	5.6%	
Angiogenesis								
PEDF_HUMAN	Pigment epithelium-derived factor precursor	46313/5.97	27	3.19	308	9	25.6%	[21]
			28	2.12	59	1	2.6%	
Proteolysis								
PSA_HUMAN	Puromycin-sensitive aminopeptidase	103211/5.49	3	2.15	83	6	6.1%	

Table 3 (continued)

Swiss Prot ID[a]	Identified Protein[a]	Theor. MW/pI[b]	SSP[c]	Av. ratio[d]	Protein score[e]	Matched peptides	Sequence coverage (%)	Bibliographic references[f]
Plasma protein								
TRFE_HUMAN	Serotransferrin precursor	77000/6.81	8	6.06	1681	50	61.9%	[25]
			9	6.21	924	52	52.3%	
			10	4.01	1746	68	61.7%	
ALBU_HUMAN	Serum albumin precursor	69321/5.92	15	6.54	1434	89	57.8%	[69]
			16	2.29	1052	42	63.4%	
			17	6.36	907	30	51.7%	
			18	7.57	928	36	56.7%	
VTDB_HUMAN	Vitamin D-binding protein precursor	52929/5.4	32	3.69	295	14	27.4%	
Non identified			34	2.23				

[a] Accession numbers of proteins and protein name from Swiss-Prot databases

[b] Theoretical molecular weight and isoelectric point obtained from Swiss-Prot and the ExPASy databases (http://au.expasy.org)

[c] Sample spot number (SSP) refers to numbering in Fig. 1

[d] Av. ratio refers to the ratio of normalized spot intensities of tumoral and non-tumoral tissues. A positive ratio indicates over-expression in the tumor, whereas a negative ratio indicates a reduced expression in the tumor

[e] Mascot score for the identified proteins based on the peptide ion score with a confidence level of at least 95% (http://www.matrixscience.com)

[f] Bibliographic reference for proteins already described in carcinogenesis or liver pathology by transcriptomic, proteomic or specific studies

be the case in 4 out of 4 patient samples as shown in Fig. 2. In the case of α-smooth muscle actin, 14-3-3 proteins and periostin, immunohistochemistry was carried out on multiple samples to confirm both the elevated expression in the tumoral liver tissue and the localization of the expression to particular cell populations (see below).

Western blot analysis of periostin expression in the same samples as those used for 2-D DIGE, confirmed that perisotin was highly expressed in four out of four tumor samples while the normal non-tumoral liver from the same patients showed undetectable periostin levels (Fig. 3). Periostin appeared as a single band of approximately 75 kDa.

Immunohistochemistry

Routine histology performed on samples of tumoral liver tissue showed typical features of peripheral cholangiocarcinoma. The surrounding non-tumoral liver tissue was in general relatively normal in appearance with only slight signs of nonspecific inflammation in a normal appearing liver parenchyma. Immunohistochemistry performed to detect three proteins that were found to be differentially expressed in the tumoral liver tissue confirmed high levels of expression of α-smooth muscle actin, 14-3-3 proteins and periostin in the cholangiocarcinoma tissue but not in the adjacent non-tumoral liver tissue in all of the samples that were examined. 14-3-3 proteins were found to be differentially expressed in the tumoral biliary cells themselves and not expressed in the tumoral stroma or in hepatocytes of the surrounding non-tumoral liver (Fig. 4a and b). Some expression was detected in normal intrahepatic biliary epithelial cells. α-Smooth muscle actin was found to be strongly expressed in myofibroblasts in fibrous stroma within the tumor and in myofibroblasts that infiltrate between the carcinoma cells (Fig. 4c and d). In non-tumoral liver tissue only low levels of α-smooth muscle actin expression were seen; however, expression was normally found in structures where it would be expected to be present, such as vascular smooth muscle cells surrounding arterioles in the portal areas. There was no evidence of fibrotic changes with associated high levels of α-smooth muscle actin-positivity in surrounding non-tumoral liver parenchyma. The extracellular matrix protein periostin was found to be highly expressed in the tumor stroma and in and around myofibroblasts present within the tumoral liver tissue (Fig. 4e and f). Periostin staining was not seen in non-tumoral liver sections from the same subjects. Taking into account the similar location of periostin and of α-smooth muscle actin which suggested that periostin was produced by activated myofibroblasts within the tumoral liver tissue, we carried out double immunostaining to colocalise these two proteins. Double immunostaining showed that stromal myofibroblasts were positive for both α-smooth muscle actin and periostin but that the periostin had a wider distribution, we believe, because it is secreted into the extracellular matrix in addition to being localised within the myofibroblasts themselves (Fig. 5a, b and c).

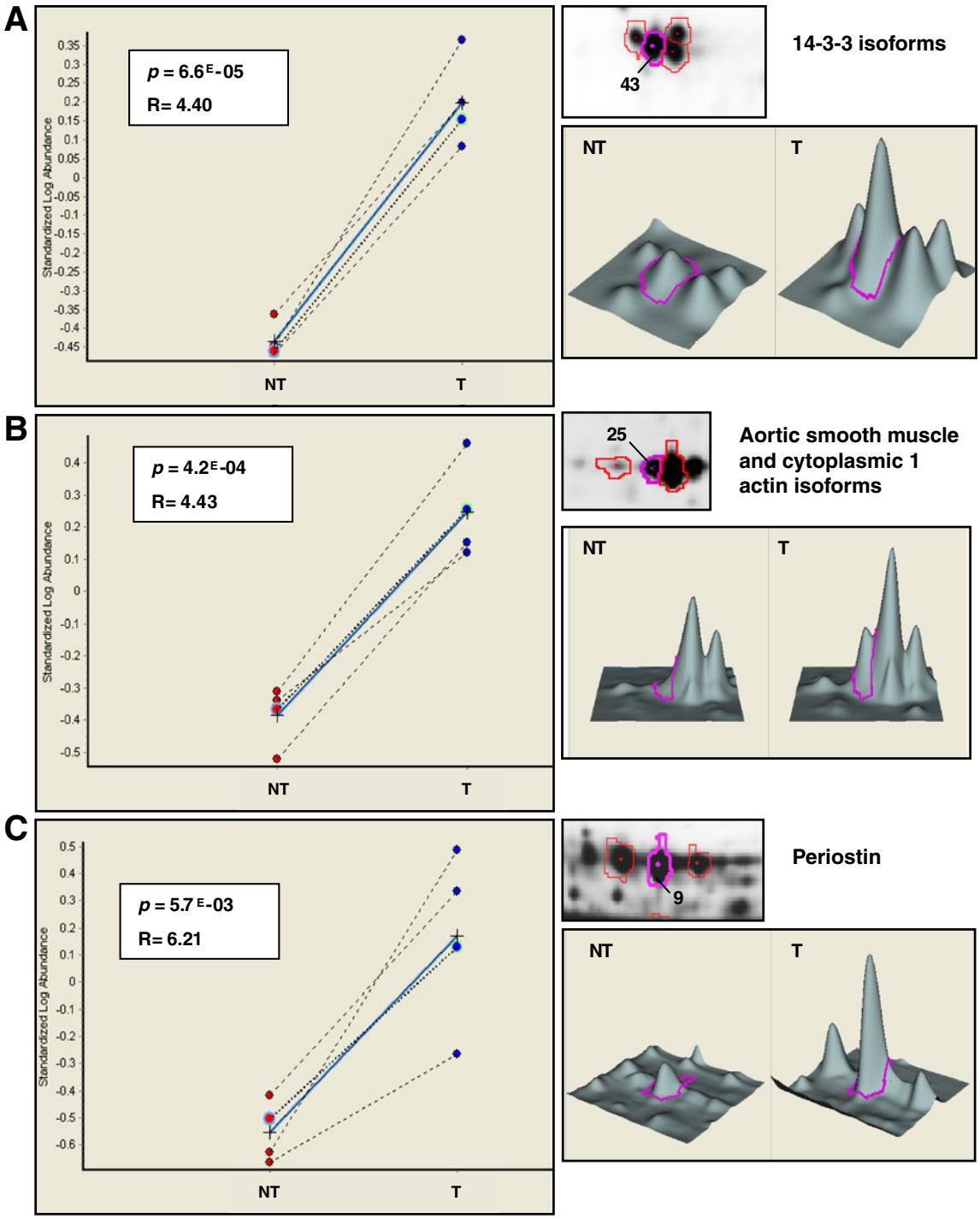

Fig. 2 Quantitative analyses illustrating 14-3-3 isoforms a, aortic smooth muscle and cytoplasmic 1 actin isoforms b and periostin c overexpression in tumoral liver (T) compared with non-tumoral liver (NT) (dotted lines and full line show the data for the 4 patients and the mean respectively). On the right, enlarged regions of 2-D gel images showing pixel volume distributions between non-tumoral and tumoral samples. 2-D DIGE analysis was performed using DeCyder software. The Cy3 to Cy5 average ratios (R) were calculated using the biological variation analysis module of DeCyder. An independent Student's test was applied to all samples, yielding a *p*-value within the 99th percentile confidence level for these three proteins

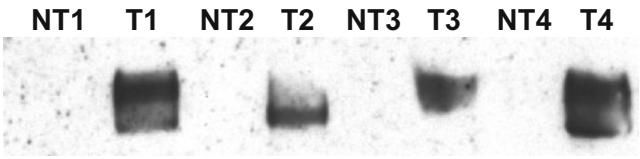

Fig. 3 Western blot for periostin in non-tumoral *(NT)* and tumoral (*T*) liver tissue from the same 4 patients used for 2-D DIGE analysis. Numbers refer to individual patients. All of the tumor samples (*T1*, *T2*, *T3*, *T4*) show very strong periostin expression at approximately 75 kDa while non-tumoral liver samples show undetectable periostin levels (*NT1*, *NT2*, *NT3*, *NT4*)

Discussion

In this study we have compared the proteome of peripheral cholangiocarcinoma to that of the surrounding non-tumoral liver tissue. This represents a novel study of differentially expressed proteins in cholangiocarcinoma which to our knowledge has not been previously reported. We have used a strategy of examining a small number of samples with tumor and control tissue from the same subject and then further analysis by immunohistochemistry and Western blotting of

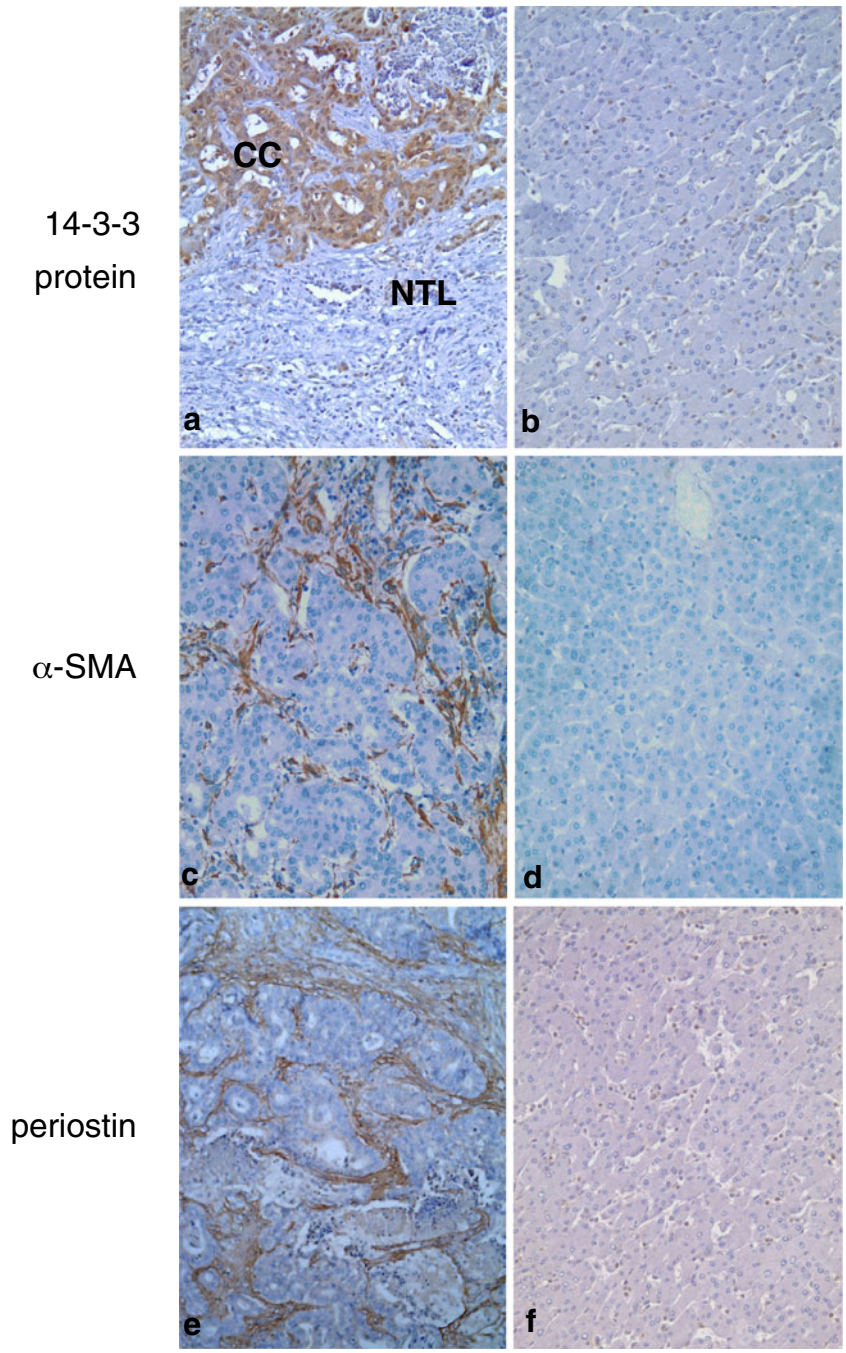

Fig. 4 Immunostaining of differentially expressed proteins in cholangiocarcinoma (a, c, e) compared to adjacent non-tumoral liver tissue (b, d, f). 14-3-3 protein staining is seen in the tumoral cells within the cholangiocarcinoma (*CC*) but not in stromal cells and non-tumoral liver tissue (NTL) (**a**). It can be seen that non-tumoral liver tissue shows no visible expression of 14-3-3 protein (**b**). Strong staining for α-smooth muscle actin is observed in stromal myofibroblasts within the tumoral tissue (**c**). α-Smooth muscle actin staining is only seen in few smooth muscle cells associated with blood vessels in the non-tumoral liver parenchyma (**d**). Periostin staining shows a similar distribution to α-smooth muscle actin staining with periostin being detected in stromal connective tissue and myofibroblasts (**e**), while in the non-tumoral liver tissue (**f**), there is no apparent staining for periostin. Magnification x200

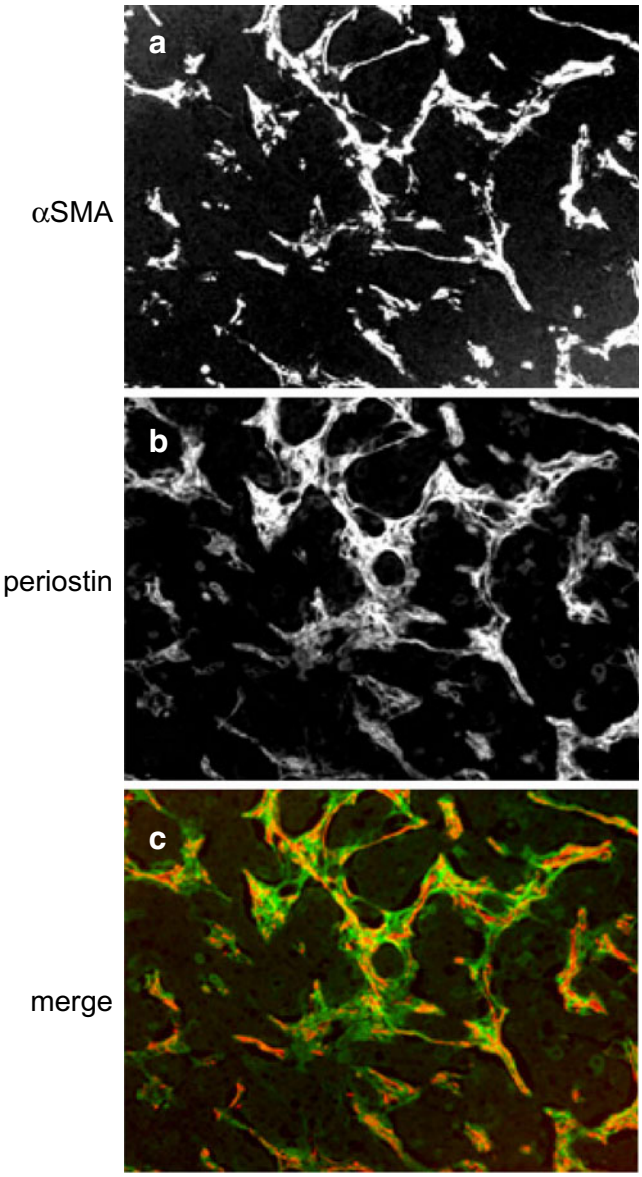

Fig. 5 Immunofluorescence comparing the distribution of α-smooth muscle actin to that of periostin. In the cholangiocarcinoma tissue, there is strong staining for α-smooth muscle actin in the stromal cells within the tumor (**a**). A similar distribution is seen with periostin staining (**b**). Merge image for the two proteins (**c**) shows that α-smooth muscle actin and periostin are colocalized in stromal cells, though periostin (*green*) has a slightly wider distribution than α-smooth muscle actin (*red*) as it is both intracellular in myofibroblasts and deposited in the extracellular matrix. Magnification x200

some of the proteins found to be differentially expressed. Cholangiocarcinoma is a relatively rare cancer and thus sample sizes tend to be small, however, we assume that by choosing the most histologically typical tumors that were on a relatively normal liver background, we have identified proteins that are consistently and significantly differently expressed between cancerous tissue and the normal liver. The analysis of 2-D gels showed a large number of differentially-expressed proteins in the tumoral liver tissue when compared to the surrounding non-tumoral and morphologically normal liver that was taken from the same patients. A number of these proteins could be predicted to play roles in tumorigenesis or tumor growth. Some of the identified proteins have been shown to be differentially expressed in experimental models or other tumor types such as colon or liver cancer ([15, 16, 25, 26]). Overall the proteins found to be over-expressed or under-expressed in tumoral tissue fell into the categories shown in Fig. 6. Over-expressed proteins largely consisted of cytoskeleton, metabolism and cell cycle, apoptosis or survival proteins, while the majority of proteins found to be under-expressed in tumor tissue were proteins involved in metabolic pathways.

Of the over-expressed proteins, those that may have a role in tumorigenesis or that have been linked to other cancers include: 60 S acidic ribosomal protein P0 over-expression which has been linked to proliferation in breast and liver cancer [27], alpha-actinin 4 which is also differentially expressed in hepatocellular carcinoma [28], annexin V which has been shown to be elevated in chemically induced hepatocarcinoma [29]; as have elongation factor 1 delta [17] and ezrin [19]. Other proteins that have also been shown to be elevated in hepatocellular carcinoma include fibrinogen gamma chain precursor [30], glutathione S transferase [31], glycerol-3-phosphate dehydrogenase [32], histone-binding protein RBBP4 [33] and nucleophosmin [34]. Lamin-A/C was elevated in sera of patients with a hepatocellular carcinoma [35]. Other proteins have been shown to be associated with different tumor types such as L-lactate dehydrogenase B chain which is elevated in lung cancer [36], niban which is over-expressed in renal tumors [37], and non-syndromic hearing impairment protein 5 which shows altered expression in colorectal cancer [38].

Of particular interest were proteins that have not yet been shown in liver cancers such as 14-3-3 proteins and periostin. 14-3-3 proteins have been shown to have roles in suppressing apoptosis or regulating cell survival ([20, 39–41]) and these may represent a novel indicator of cancer transformation in hepatocytes or biliary epithelium. In addition to its role in regulation of apoptosis, 14-3-3 sigma protein, also known as stratifin, is now known to be secreted via exosomes and induces expression of the matrix metalloproteinases, MMP-1 and MMP-3. This may also link its over-expression to increased cell migration or capacity for invasion [42].

Periostin is a secreted protein that has integrin binding sites and has been shown to be expressed by tumor cells and tumor stroma in melanoma and colon cancer ([23, 24]). We have shown elevated expression in cholangiocarcinoma and this expression was then localised to the tumor stroma (myofibroblasts) by immunohistochemistry. Recent exami-

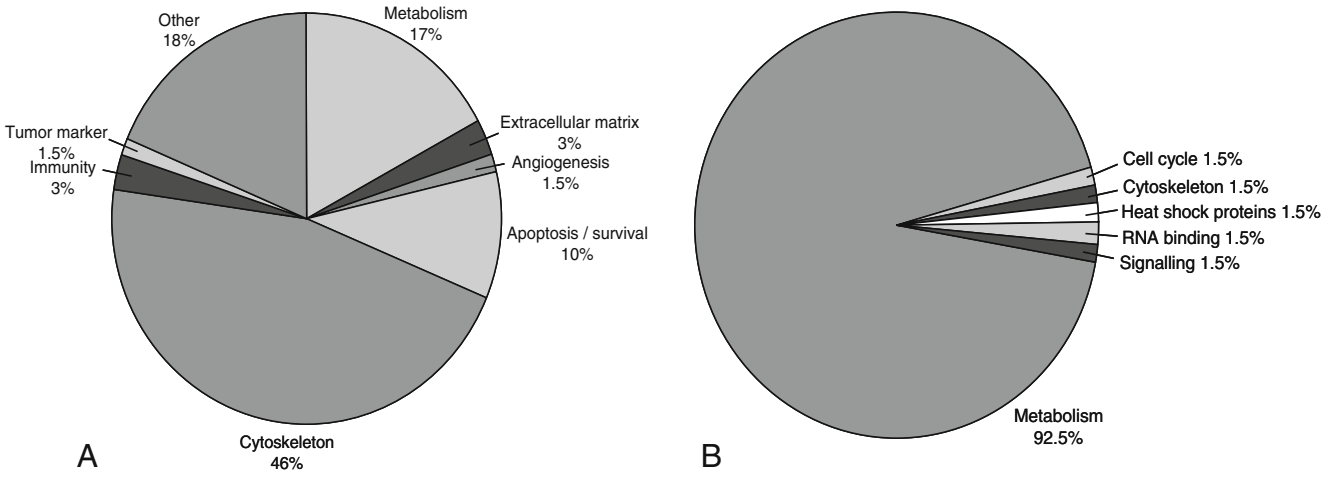

Fig. 6 Diagrammatic representation of the functions of proteins that were identified as either over-expressed (**a**) or under-expressed (**b**) in the tumoral compared to non-tumoral liver tissue. Assignments were made on the basis of information provided in the SWISS-PROT website (www.expasy.ch)

nation of fibroblasts isolated from cholangiocarcinoma has shown that these cells are capable of producing periostin and that high levels of periostin production correlate with poor prognosis [9]. Further studies using in situ hybridization for periostin mRNA expression may clarify whether periostin is expressed in cholangiocarcinoma uniquely in the tumor-associated myofibroblasts. It has been suggested recently that the stroma may play an important role in tumor growth and progression and periostin may be a novel candidate protein for regulation of cancer cell behaviour. Periostin has been shown to induce cell migration and also epithelial-mesenchymal transition in pancreatic cancer cells [43], thus it may represent a novel mediator of tumor growth in cholangiocarcinoma. In addition, periostin has been reported to be elevated in serum of some patients with cancers including thymoma and non-small cell lung carcinoma [44]. The detection of periostin or other over-expressed proteins such as 14-3-3 preoteins in serum may therefore prove to be useful markers for detection of malignancy.

In view of the fact that cholangiocarcinoma has shown a recent increase in incidence, along with the difficulty in early diagnosis, we believe that studies such as this may be useful in identifying proteins that may have a role in cancer development or progression. The use of differentially expressed proteins such as those identified in this study may provide the possibility of finding markers for detection of cholangiocarcinoma, although this is complicated by the fact that some of these proteins are differentially expressed in other malignancies. Identifying a unique pattern of expression or the possibility that these proteins may represent serum or bile markers should also be considered. Further studies are required to examine possible links between these proteins and disease outcome or prognosis as well as comparisons between the proteome of hepatocellular carcinoma, non-malignant disease of the liver (cirrhosis) and stroma of metastatic tumors.

Acknowledgements This work was supported in part by a grant from the University of Limoges (Contrat Renforcé Recherche). Ian A. Darby was supported in part by the Australian Academy of Sciences (2007), and the University of Limoges (Invited Professor, 2008). We thank Dr. R. Julien (Université de Limoges, Faculté des Sciences et Techniques) for his helpful advice.

References

1. Bonney GK, Craven RA, Prasad R, Melcher AF, Selby PJ, Banks RE (2008) Circulating markers of biliary malignancy: opportunities in proteomics? Lancet Oncol 9:149–158
2. Kaewpitoon N, Kaewpitoon SJ, Pengsaa P, Sripa B (2008) Opisthorchis viverrini: the carcinogenic human liver fluke. World J Gastroenterol 14:666–674
3. Terada T, Makimoto K, Terayama N, Suzuki Y, Nakanuma Y (1996) Alpha-smooth muscle actin-positive stromal cells in cholangiocarcinomas, hepatocellular carcinomas and metastatic liver carcinomas. J Hepatol 24:706–712
4. Okamura N, Yoshida M, Shibuya A, Sugiura H, Okayasu I, Ohbu M (2005) Cellular and stromal characteristics in the scirrhous hepatocellular carcinoma: comparison with hepatocellular carcinomas and intrahepatic cholangiocarcinomas. Pathol Int 55:724–731
5. Terada T, Okada Y, Nakanuma Y (1996) Expression of immunoreactive matrix metalloproteinases and tissue inhibitors of matrix metalloproteinases in human normal livers and primary liver tumors. Hepatology (Baltim Md) 23:1341–1344
6. Guyot C, Lepreux S, Darby IA, Desmoulière A (2007) The biology of tumor stroma. In: Alison MR (ed) The cancer handbook, 2nd edn. John Wiley & Sons, Chichester, pp 155–167
7. Schumacher B, Mondry J, Thiel P, Weyand M, Ottmann C (2010) Structure of the p53 C-terminus bound to 14-3-3: implications for stabilization of the p53 tetramer. FEBS Lett 584:1443–1448
8. Tsujino T, Seshimo I, Yamamoto H et al (2007) Stromal myofibroblasts predict disease recurrence for colorectal cancer. Clin Cancer Res 13:2082–2090
9. Utispan K, Thuwajit P, Abiko Y et al (2010) Gene expression profiling of cholangiocarcinoma-derived fibroblast reveals alter-

ations related to tumor progression and indicates periostin as a poor prognostic marker. Mol Cancer 9:13
10. Friedman DB, Hill S, Keller JW et al (2004) Proteome analysis of human colon cancer by two-dimensional difference gel electrophoresis and mass spectrometry. Proteomics 4:793–811
11. Neuhoff V, Arold N, Taube D, Ehrhardt W (1988) Improved staining of proteins in polyacrylamide gels including isoelectric focusing gels with clear background at nanogram sensitivity using Coomassie Brilliant Blue G-250 and R-250. Electrophoresis 9:255–262
12. Jelski W, Zalewski B, Szmitkowski M (2008) Alcohol dehydrogenase (ADH) isoenzymes and aldehyde dehydrogenase (ALDH) activity in the sera of patients with liver cancer. J Clin Lab Anal 22:204–209
13. Yang Y, Ding L, Li S (1990) The immunohistochemistry and in situ cDNA-mRNA hybridization of carbamyl phosphate synthetase I in enzyme-altered liver cells during carcinogenesis. Proc Chin Acad Med Sci Peking Union Med Coll 5:13–18
14. Li T, Yang W, Li M et al (2008) Expression of selenium-binding protein 1 characterizes intestinal cell maturation and predicts survival for patients with colorectal cancer. Mol Nutr Food Res 52:1289–1299
15. Kim H, Kang HJ, You KT et al (2006) Suppression of human selenium-binding protein 1 is a late event in colorectal carcinogenesis and is associated with poor survival. Proteomics 6:3466–3476
16. Rousseau B, Menard L, Haurie V et al (2007) Overexpression and role of the ATPase and putative DNA helicase RuvB-like 2 in human hepatocellular carcinoma. Hepatology (Baltim Md) 46:1108–1118
17. Shuda M, Kondoh N, Tanaka K et al (2000) Enhanced expression of translation factor mRNAs in hepatocellular carcinoma. Anticancer Res 20:2489–2494
18. Cook JA, Chuang EY, Tsai MH et al (2006) Radiation-induced changes in gene-expression profiles for the SCC VII tumor cells grown in vitro and in vivo. Antioxid Redox Signal 8:1263–1272
19. Zhang Y, Hu MY, Wu WZ et al (2006) The membrane-cytoskeleton organizer ezrin is necessary for hepatocellular carcinoma cell growth and invasiveness. J Cancer Res Clin Oncol 132:685–697
20. Masters SC, Yang H, Datta SR, Greenberg ME, Fu H (2001) 14-3-3 inhibits Bad-induced cell death through interaction with serine-136. Mol Pharmacol 60:1325–1331
21. Matsumoto K, Ishikawa H, Nishimura D, Hamasaki K, Nakao K, Eguchi K (2004) Antiangiogenic property of pigment epithelium-derived factor in hepatocellular carcinoma. Hepatology (Baltim Md) 40:252–259
22. Shao R, Bao S, Bai X et al (2004) Acquired expression of periostin by human breast cancers promotes tumor angiogenesis through up-regulation of vascular endothelial growth factor receptor 2 expression. Mol Cell Biol 24:3992–4003
23. Tilman G, Mattiussi M, Brasseur F, van Baren N, Decottignies A (2007) Human periostin gene expression in normal tissues, tumors and melanoma: evidences for periostin production by both stromal and melanoma cells. Mol Cancer 6:80
24. Bao S, Ouyang G, Bai X et al (2004) Periostin potently promotes metastatic growth of colon cancer by augmenting cell survival via the Akt/PKB pathway. Cancer Cell 5:329–339
25. Ioannou GN, Weiss NS, Kowdley KV (2007) Relationship between transferrin-iron saturation, alcohol consumption, and the incidence of cirrhosis and liver cancer. Clin Gastroenterol Hepatol 5:624–629
26. Loilome W, Yongvanit P, Wongkham C et al (2006) Altered gene expression in Opisthorchis viverrini-associated cholangiocarcinoma in hamster model. Mol Carcinog 45:279–287
27. Chang TW, Chen CC, Chen KY, Su JH, Chang JH, Chang MC (2008) Ribosomal phosphoprotein P0 interacts with GCIP and overexpression of P0 is associated with cellular proliferation in breast and liver carcinoma cells. Oncogene 27:332–338
28. Nishiyama M, Ozturk M, Frohlich M, Mafune K, Steele G Jr, Wands JR (1990) Expression of human alpha-actinin in human hepatocellular carcinoma. Cancer Res 50:6291–6294
29. Fella K, Gluckmann M, Hellmann J, Karas M, Kramer PJ, Kroger M (2005) Use of two-dimensional gel electrophoresis in predictive toxicology: identification of potential early protein biomarkers in chemically induced hepatocarcinogenesis. Proteomics 5:1914–1927
30. Chan KY, Lai PB, Squire JA et al (2006) Positional expression profiling indicates candidate genes in deletion hotspots of hepatocellular carcinoma. Mod Pathol 19:1546–1554
31. Pires PW, Furtado KS, Justullin LA Jr, Rodrigues MA, Felisbino SL, Barbisan LF (2008) Chronic ethanol intake promotes double gluthatione S-transferase/transforming growth factor-alpha-positive hepatocellular lesions in male Wistar rats. Cancer Sci 99:221–228
32. Mayer D, Metzger C, Leonetti P, Beier K, Benner A, Bannasch P (1998) Differential expression of key enzymes of energy metabolism in preneoplastic and neoplastic rat liver lesions induced by N-nitrosomorpholine and dehydroepiandrosterone. Int J Cancer 79:232–240
33. Song H, Xia SL, Liao C et al (2004) Genes encoding Pir51, Beclin 1, RbAp48 and aldolase b are up or down-regulated in human primary hepatocellular carcinoma. World J Gastroenterol 10:509–513
34. Yun JP, Miao J, Chen GG et al (2007) Increased expression of nucleophosmin/B23 in hepatocellular carcinoma and correlation with clinicopathological parameters. Br J Cancer 96:477–484
35. Li L, Chen SH, Yu CH, Li YM, Wang SQ (2008) Identification of hepatocellular-carcinoma-associated antigens and autoantibodies by serological proteome analysis combined with protein microarray. J Proteome Res 7:611–620
36. Chen Y, Zhang H, Xu A et al (2006) Elevation of serum l-lactate dehydrogenase B correlated with the clinical stage of lung cancer. Lung Cancer 54:95–102
37. Adachi H, Majima S, Kon S et al (2004) Niban gene is commonly expressed in the renal tumors: a new candidate marker for renal carcinogenesis. Oncogene 23:3495–3500
38. Kim MS, Chang X, Yamashita K et al (2008) Aberrant promoter methylation and tumor suppressive activity of the DFNA5 gene in colorectal carcinoma. Oncogene 27:3624–3634
39. Datta SR, Katsov A, Hu L et al (2000) 14-3-3 proteins and survival kinases cooperate to inactivate BAD by BH3 domain phosphorylation. Mol Cell 6:41–51
40. Li Z, Zhao J, Du Y et al (2008) Down-regulation of 14-3-3zeta suppresses anchorage-independent growth of lung cancer cells through anoikis activation. Proc Natl Acad Sci USA 105:162–167
41. Fan T, Li R, Todd NW et al (2007) Up-regulation of 14-3-3zeta in lung cancer and its implication as prognostic and therapeutic target. Cancer Res 67:7901–7906
42. Chavez-Munoz C, Morse J, Kilani R, Ghahary A (2008) Primary human keratinocytes externalize stratifin protein via exosomes. J Cell Biochem 104:2165–2173
43. Kanno A, Satoh K, Masamune A et al (2008) Periostin, secreted from stromal cells, has biphasic effect on cell migration and correlates with the epithelial to mesenchymal transition of human pancreatic cancer cells. Int J Cancer 122:2707–2718
44. Sasaki H, Yu CY, Dai M et al (2003) Elevated serum periostin levels in patients with bone metastases from breast but not lung cancer. Breast Cancer Res Treat 77:245–252
45. Krupenko SA, Oleinik NV (2002) 10-formyltetrahydrofolate dehydrogenase, one of the major folate enzymes, is down-

regulated in tumor tissues and possesses suppressor effects on cancer cells. Cell Growth Differ 13:227–236
46. Praml C, Savelyeva L, Schwab M (2003) Aflatoxin B1 aldehyde reductase (AFAR) genes cluster at 1p35-1p36.1 in a region frequently altered in human tumour cells. Oncogene 22:4765–4773
47. Mielczarek M, Chrzanowska A, Scibior D et al (2006) Arginase as a useful factor for the diagnosis of colorectal cancer liver metastases. Int J Biol Markers 21:40–44
48. Goss SJ (1986) Characterization of cystathionine synthase as a selectable, liver-specific trait in rat hepatomas. J Cell Sci 82:309–320
49. Graziano C, Comin CE, Crisci C et al (2008) Functional polymorphisms of the microsomal epoxide hydrolase gene: A reappraisal on a early-onset lung cancer patients series. Lung Cancer
50. Lu SC, Mato JM (2008) S-Adenosylmethionine in cell growth, apoptosis and liver cancer. J Gastroenterol Hepatol 23(Suppl 1): S73–77
51. Luk JM, Lam CT, Siu AF et al (2006) Proteomic profiling of hepatocellular carcinoma in Chinese cohort reveals heat-shock proteins (Hsp27, Hsp70, GRP78) up-regulation and their associated prognostic values. Proteomics 6:1049–1057
52. Liou JY, Ghelani D, Yeh S, Wu KK (2007) Nonsteroidal anti-inflammatory drugs induce colorectal cancer cell apoptosis by suppressing 14-3-3epsilon. Cancer Res 67:3185–3191
53. Matta A, Bahadur S, Duggal R, Gupta SD, Ralhan R (2007) Over-expression of 14-3-3zeta is an early event in oral cancer. BMC Cancer 7:169
54. Bei R, Masuelli L, Trono P et al (2007) The ribosomal P0 protein induces a spontaneous immune response in patients with head and neck advanced stage carcinoma that is not dependent on its overexpression in carcinomas. Int J Oncol 31:1301–1308
55. Gulubova MV (2004) Collagen type IV, laminin, alpha-smooth muscle actin (alphaSMA), alpha1 and alpha6 integrins expression in the liver with metastases from malignant gastrointestinal tumours. Clin Exp Metastasis 21:485–494
56. She R, Szakacs J (2005) Carcinosarcoma of the liver: a case report and review of the literature. Arch Pathol Lab Med 129:790–793
57. Neubauer K, Baruch Y, Lindhorst A, Saile B, Ramadori G (2003) Gelsolin gene expression is upregulated in damaged rat and human livers within non-parenchymal cells and not in hepatocytes. Histochem Cell Biol 120:265–275
58. Chiu CC, Huang GT, Chou SH et al (2007) Characterization of cytokeratin 19-positive hepatocyte foci in the regenerating rat liver after 2-AAF/CCl4 injury. Histochem Cell Biol 128:217–226
59. Sun S, Xu MZ, Poon RT, Day PJ, Luk JM (2009) Circulating Lamin B1 (LMNB1) Biomarker Detects Early Stages of Liver Cancer in Patients. J Proteome Res
60. Perlmutter DH (2006) Pathogenesis of chronic liver injury and hepatocellular carcinoma in alpha-1-antitrypsin deficiency. Pediatr Res 60:233–238
61. Jacob A, Zhou M, Wu R, Halpern VJ, Ravikumar TS, Wang P (2007) Pro-inflammatory cytokines from Kupffer cells down-regulate hepatocyte expression of adrenomedullin binding protein-1. Biochim Biophys Acta 1772:766–772
62. Kim H (2008) DNA repair Ku proteins in gastric cancer cells and pancreatic acinar cells. Amino Acids 34:195–202
63. Avila MA, Berasain C, Torres L et al (2000) Reduced mRNA abundance of the main enzymes involved in methionine metabolism in human liver cirrhosis and hepatocellular carcinoma. J Hepatol 33:907–914
64. Fan Y, Shimizu T, Yamada T et al (2008) Development of glutathione S-transferase-P-negative foci accompanying nuclear factor-erythroid 2-related factor 2 expression during early stage of rat hepatocarcinogenesis. Cancer Sci 99:497–501
65. Noguchi Y, Yoshikawa T, Marat D et al (1999) Tumor-associated metabolic alterations in patients with gastric and esophageal cancer. Hepatogastroenterology 46:555–560
66. Krull NB, Gressner AM (1992) Differential expression of keratan sulphate proteoglycans fibromodulin, lumican and aggrecan in normal and fibrotic rat liver. FEBS Lett 312:47–52
67. Baril P, Gangeswaran R, Mahon PC et al (2007) Periostin promotes invasiveness and resistance of pancreatic cancer cells to hypoxia-induced cell death: role of the beta4 integrin and the PI3k pathway. Oncogene 26:2082–2094
68. Siriwardena BS, Kudo Y, Ogawa I et al (2006) Periostin is frequently overexpressed and enhances invasion and angiogenesis in oral cancer. Br J Cancer 95:1396–1403
69. D'Errico A, Baccarini P, Fiorentino M et al (1996) Histogenesis of primary liver carcinomas: strengths and weaknesses of cytokeratin profile and albumin mRNA detection. Hum Pathol 27:599–604